

Marquette University

e-Publications@Marquette

Chemistry Faculty Research and Publications

Chemistry, Department of

9-2002

Crown Ether-Modified Clays and their Polystyrene Nanocomposites

Hongyang Jao
Marquette University

Jin Zhu
Marquette University

Alexander B. Morgan
National Institute of Standards and Technology

Charles A. Wilkie
Marquette University, charles.wilkie@marquette.edu

Follow this and additional works at: https://epublications.marquette.edu/chem_fac

 Part of the [Chemistry Commons](#)

Recommended Citation

Jao, Hongyang; Zhu, Jin; Morgan, Alexander B.; and Wilkie, Charles A., "Crown Ether-Modified Clays and their Polystyrene Nanocomposites" (2002). *Chemistry Faculty Research and Publications*. 29.
https://epublications.marquette.edu/chem_fac/29

Crown Ether-Modified Clays and Their Polystyrene Nanocomposites

HONGYANG YAO,¹ JIN ZHU,¹ ALEXANDER B. MORGAN,^{2*}
and CHARLES A. WILKIE¹

¹Department of Chemistry
Marquette University
P.O. Box 1881, Milwaukee, WI 53201

²Fire Science Division
Building and Fire Research Laboratory
National Institute of Standards and Technology
Gaithersburg, MD 20899[†]

Crown ether-modified clays were obtained by the combination of sodium and potassium clays with crown ethers and cryptands. Polystyrene nanocomposites were prepared by bulk polymerization in the presence of these clays. The structures of nanocomposites were characterized by X-ray diffraction and transmission electron microscopy. Their thermal stability and flame retardancy were measured by thermogravimetric analysis and cone calorimetry, respectively. Nanocomposites can be formed only from the potassium clays; apparently the sodium clays are not sufficiently organophilic to enable nanocomposite formation. The onset temperature of the degradation is higher for the nanocomposites compared to virgin polystyrene, and the peak heat release rate is decreased by 25% to 30%.

INTRODUCTION

Polymer-clay nanocomposites have been extensively studied because of their enhanced mechanical properties (1–3), thermal stability and fire retardancy (4, 5), gas barrier properties (6), ionic conductivity (7), etc., relative to the neat polymers. It is essential that there is compatibility between the polymer and the clay to obtain well-dispersed materials. Since the natural clay is highly hydrophilic, it is important to improve its organophilicity so that it will be compatible with organic polymers.

There are two methods to modify the sodium clay: exchange the sodium cations within the gallery space with quaternary organic cations, like ammonium or phosphonium salts (8, 9); or directly modify the clay layers, using organic coupling agents, such as silane coupling agents (10).

Another possible modification is to render the alkali metal cation organophilic by complexation with a crown ether. Crown ether-modified clay was first reported in 1978 by Ruiz-Hitzky and Casal, who reported on the stability, ion-exchange properties and other behavior of the nanocomposite materials (11). The ionic conductivity of crown ether-phylosilicates is several orders of magnitude higher than that of the parent silicate (12). More recently, Gilman reported

that crown ether-modified clays can be well dispersed in polyamide-6 (PA-6) and form nanocomposites (13).

In this paper, we report the preparation of a number of crown ether-modified clays and their polystyrene (PS) nanocomposites, prepared by an in-situ bulk polymerization. These materials have been characterized by X-ray diffraction (XRD) transmission electron microscopy (TEM) thermogravimetric analysis (TGA) and cone calorimetry.

EXPERIMENTAL[†]

Materials. The sodium clay was provided by Southern Clay Products, Inc.; most of the other chemicals were obtained from the Aldrich Chemical Co. and used as obtained, including 18-Crown-6, Benzo-18-crown-6, Dibenzo-18-crown-6, *cis*-Dicyclohexano-18-

*Current Address: The Dow Chemical Company, Nanomaterials Group, Midland, MI 48674.

[†]It is the policy of the National Institute of Standards and Technology to use the International System of Units (metric units) in its technical communications. However, in this document, other units are used to conform to the publisher's style. Further, this work was carried out by the National Institute of Standards and Technology (NIST), an agency of the U.S. government, and all NIST data in this paper, by statute, is not subject to copyright in the United States.

[‡]Certain commercial equipment, instruments, materials or companies are identified in this paper in order to adequately specify the experimental procedure. This in no way implies endorsement or recommendation by NIST.

crown-6, [2.2.2] cryptand (4,7,13,16,21,24-hexaoxa-1,10-diaza-bicyclo[8.8.8]-hexacosane), styrene, and 2,2'-azobisisobutyronitrile (AIBN).

Instrumentation. XRD was performed using a Rigaku powder diffractometer, with a Cu tube source ($\lambda = 1.54 \text{ \AA}$) operated at 1 kW. TEM images were obtained at 120 kV, at low dose conditions, with a Phillips 400T electron microscope. The samples were ultramicrotomed with a diamond knife on a Leica Ultracut UCT microtome at room temperature to give 70-nm-thick sections. The sections were transferred from water to carbon-coated (type B) Cu grids of 200 mesh. The contrast between the layered silicates and the polymer phase was sufficient for imaging, so no heavy metal staining of sections prior to imaging is required. TGA was carried out using a Cahn model 131 in inert atmosphere at a heating rate of 10°C per minute. All TGA runs are the average of at least two and most often three determinations; temperatures are reproduced to $\pm 3^\circ\text{C}$ while the error bars on the fraction of non-volatile residue is $\pm 3\%$. Cone samples were prepared by compression molding the sample (25–35 g) into square plaques, using a heated press. Cone calorimetry was performed using a Stanton-Redcroft/PL Thermal Sciences instruments according to ASTM E 1354-92 at an incident flux of 50 kW/m^2 using a cone shaped heater. Exhaust flow was set at 24 L/s and the spark was continuous until the sample ignited. All samples were run in duplicate and the average value is reported; typical results from cone calorimetry are reproducible to within about $\pm 10\%$ (14). Infrared spectroscopy was carried out on a Matteson Galaxy spectrometer.

Synthesis of potassium clay. About 10 g of sodium clay was suspended in 1000 mL of distilled water by stirring overnight, and then a solution of 11.2 g of KCl in 300 mL of water was added to the suspension, and the mixture was stirred for 3 days. About 500 mL of ethanol was added, and the mixture was allowed to stand for 1 day. The mixture was filtered, and the clay was collected, dried and ground to a powder.

Syntheses of crown ether-modified clays. The inorganic clay (Na^+ , K^+) was dispersed in distilled water ($\sim 1/100$, by weight) by stirring overnight in a beaker; then a 1–3 % by volume solution of crown ether in acetone ($\sim 150 \text{ mmol}/100 \text{ g}$, crown ether/clay) was added slowly to the suspension. The mixture was stirred for 2 h at room temperature, 2 h at about 45°C , and finally overnight at room temperature. The mixture was filtered and the clay was collected and dried in a vacuum oven. Infrared spectroscopy showed the presence of the crown ether; typically the C-H stretching vibration is sufficient to show the presence of the crown ether, but other infrared bands, such as C-O, etc., can also be observed. The clay was ground to a powder and characterized by XRD.

Alternate synthesis of potassium-complexed clay. The sodium clay was dispersed in distilled water ($\sim 1/100$, wt/wt) by stirring overnight in a beaker, then an 1–3% solution of potassium iodide-crown

ether complex in water (the complex was prepared by mixing KI with crown ether in water) was added dropwise to the suspension. A clay quickly precipitated; XRD results show a d-spacing typical for a potassium and not a sodium clay. The potassium ion – crown complex replaces the sodium ion in the clay and leaves sodium iodide in solution. Stirring of the mixture was continued for an additional 24 h at room temperature, and then the mixture was filtered and the clay was collected and dried in a vacuum oven.

Preparation of the polystyrene nanocomposites. About 1 wt% of crown ether-modified clay was dispersed in styrene (1/100, by weight, crown ether/styrene) by stirring overnight. AIBN (1/100, wt/wt, AIBN/styrene) was added to the mixture, and the temperature was maintained at $\sim 80^\circ\text{C}$ for a few hours while stirring, and at $\sim 120^\circ\text{C}$ overnight to complete the polymerization. The product was dried in a vacuum oven at $\sim 100^\circ\text{C}$ for 24 h. This synthetic scheme is quite similar to that which has been previously reported for PS-clay nanocomposites prepared from organically modified clays (5). Samples for cone calorimetry contained 3 wt% clay.

RESULTS AND DISCUSSION

Crown ethers and cryptands have high binding capacities for inorganic cations, such as Na^+ , K^+ , etc. These complexes have high organophilicity and can be dissolved in organic solvents. This organophilicity suggests another possible procedure for the formation of nanocomposites, using the crown ether-modified clays. The crown ethers and cryptand used in this study are shown in Fig. 1.

Different crown ethers have different binding capacity with the same cation, owing to the size of the cavity. The complexation constant reflects the binding ability between the cation and the crown ether. The larger the constant, the greater the selectivity for that cation. Some of the complexation constants are shown in the Table 1 (15). Since the size of potassium ion is more suitable for the cavity of 18-crown-6, the sodium clay has been converted to potassium clay.

Two techniques are required to prove the formation of a nanocomposite, XRD, in which an increase in the d-spacing indicates an expansion of the gallery space, and TEM, which provides an actual view of the orientation of the polymer and clay. Nanocomposites may be described as either intercalated, in which the registry between the layers is maintained, but the d-spacing has increased when compared to the virgin clay, or exfoliated, in which this registry is lost and the peak in the XRD is absent. The absence of an XRD peak can be caused by disorder in the clay, thus the loss of registry, or a very large d-spacing, which cannot be measured by normal wide-angle XRD. If the clay has maintained its order in the final nanocomposite, then it should be observable by small angle XRD (2θ less than 1°). There are examples in which the d-spacing has actually decreased relative to that

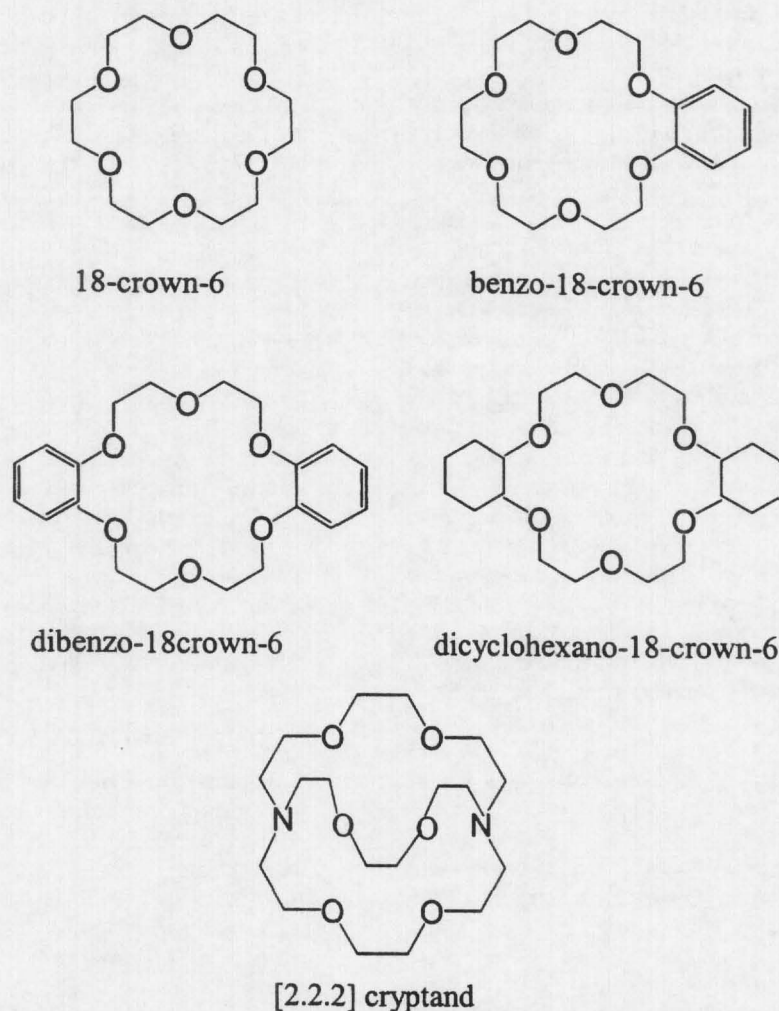


Fig. 1. The structures of crown ethers and cryptand.

of the clay, owing to decomposition of the ammonium salt during the preparation, yet the TEM shows the presence of an intercalated material (16). It is essential to have both XRD and TEM data in order to characterize a nanocomposite.

XRD measurement. The XRD data are shown in Table 2. It can be seen that the d-spacing of crown ether-modified potassium clays increases to 1.8–1.9 nm from 1.2 nm, and those of sodium clays to 1.5–1.7 nm from 1.1 nm. This clearly indicates that the crown ether or cryptand does complex with both potassium or sodium ion and effect an expansion of the d-spacing.

All of the sodium clay-PS materials show no significant change in the d-spacing, except for that of

[2.2.2]cryptand, which shows partial intercalation—a small peak at 4.7 nm in Fig. 2. For the potassium salts, both benzo-18-crown-6 and dibenzo-18-crown-6 show a large peak at the same position as in the clay and a smaller peak at larger d-spacing; this must indicate that some partial intercalation has occurred. In the case of *cis*-dicyclohexano-18-crown-6, the peak due to the clay has entirely vanished and is replaced by a peak at 7.7 nm, probably indicative of complete intercalation. The XRD curve is shown in Fig. 3.

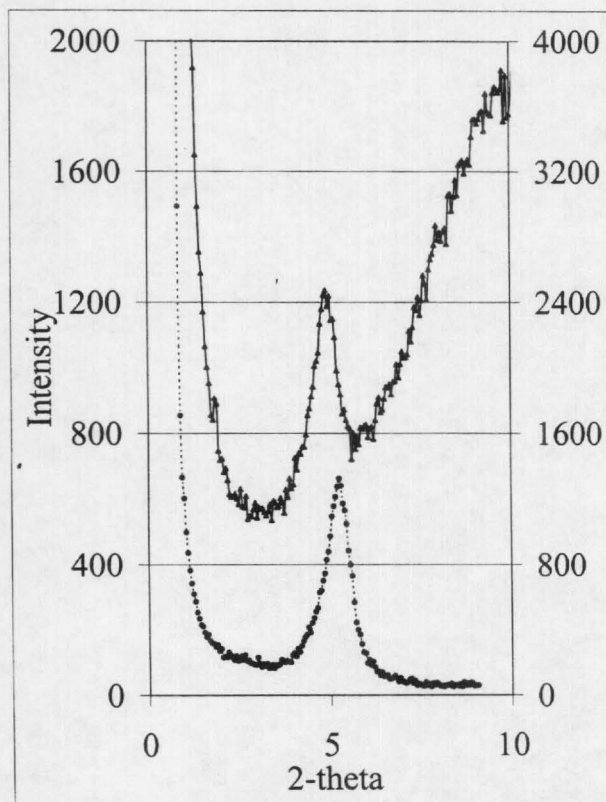
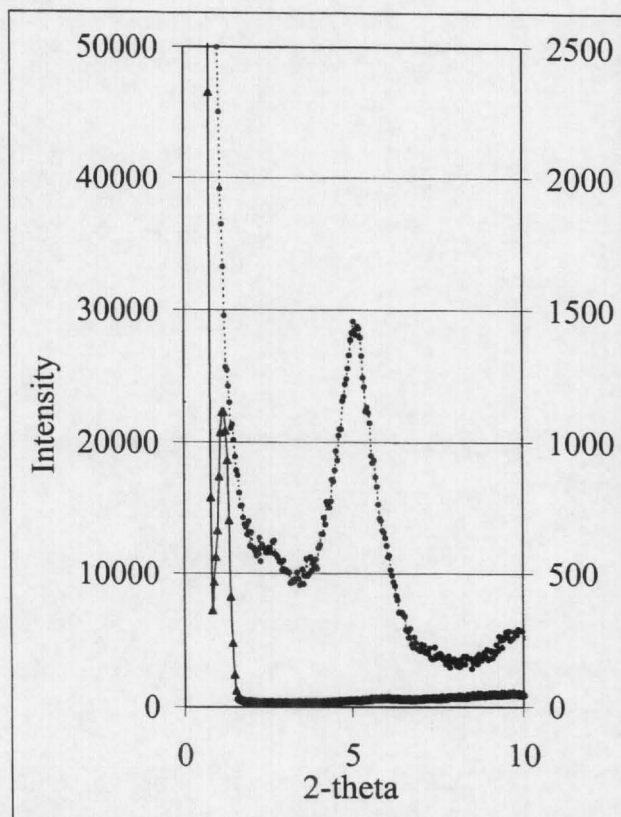
The intercalation of PS into the clay may be explained by the complexation constant between the crown ether and the cation. The larger is the complexation constant, the stronger will be the complex with the metal ion and the more organophilic the clay

Table 1. Complexation Constants of Crown Ether With Cations (15)

| Crown ether | 18-crown-6 | | Benzo-18-crown-6 | | Dibenzo-18-crown-6 | | Dicyclohexano-18-crown-6 | | [2.2.2] Cryptand | |
|-------------|-----------------|----------------|------------------|----------------|--------------------|----------------|--------------------------|----------------|------------------|----------------|
| Cations | Na ⁺ | K ⁺ | Na ⁺ | K ⁺ | Na ⁺ | K ⁺ | Na ⁺ | K ⁺ | Na ⁺ | K ⁺ |
| Log K | 4.35 | 6.08 | 4.3 | 5.3 | 4.4 | 5.0 | 4.08 | 6.01 | 8.0 | 10.6 |

Table 2. The d-Spacings of Clays Modified With Crown Ethers and Their Blends.

| Clays | d_{001} of clay (nm) | d_{001} of PS-clay (nm) |
|--|------------------------|---------------------------|
| Na ⁺ -clay | 1.0–1.2 | 1.1 |
| <i>cis</i> -Dicyclohexano-18-crown-6 Na ⁺ -Clay | 1.7 | 1.8 |
| Benzo-18-crown-6 Na ⁺ -Clay | 1.5 | 1.6 |
| Dibenzo-18-crown-6 Na ⁺ -Clay | 1.8 | 1.9 |
| [2.2.2]-Cryptand Na ⁺ -clay | 1.7 | 1.8, 4.7 (small) |
| K ⁺ -clay | 1.2 | Not measured |
| 18-crown-6 | 1.4 | 1.4, 6.5 (small) |
| <i>cis</i> -Dicyclohexano-18-crown-6 K ⁺ -Clay | 1.9 | 7.7 |
| Benzo-18-crown-6 K ⁺ -Clay | 1.8 | 1.8, 4.7 (small) |
| Dibenzo-18-crown-6 K ⁺ -clay | 1.9 | 1.9, 7.2 (small) |
| [2.2.2]-Cryptand K ⁺ -clay | 1.7 | 1.8 |

**Fig. 2.** XRD of [2.2.2] cryptand modified sodium clay, bottom, and the PS nanocomposite, top.**Fig. 3.** XRD of *cis*-Dicyclohexano-18-crown-6 (DCHCE) modified potassium clay, top, and the PS nanocomposite, bottom.

gallery space will become. The constants for sodium are smaller than those of potassium, and there is no expansion of the d-spacing for the sodium clays. The lack of nanocomposite formation for sodium clays may be attributed either to the poor complexation, leading to a still somewhat hydrophilic clay, or to the smaller d-spacing for the sodium clay, preventing access of the polymer to the gallery space, or both factors may be important. The dicyclohexano crown has the highest complexation constant of the crown ethers, and this appears to be completely intercalated. There does appear to be a relationship between the constant and the state of the clay-polymer mixture. The [2.2.2] cryptand-modified clay also forms a partially intercalated structure, probably because of the high complexation constant. It has been reported that the 18-crown-6 sodium clay dispersed well in PA-6 (13). This may be attributed to the more polar nature of PA-6 relative to PS.

TEM image. The dispersion of the clay is best observed by TEM and the images of the PS nanocomposites formed from *cis*-dicyclohexano-18-crown-6 modified potassium clay and [2.2.2] cryptand modified sodium clay are shown in Fig. 4 and Fig. 5. These images show a clearly intercalated structure for dicyclohexano-18-crown-6 potassium clay and a partially dispersed structure for the cryptand sodium clay. It

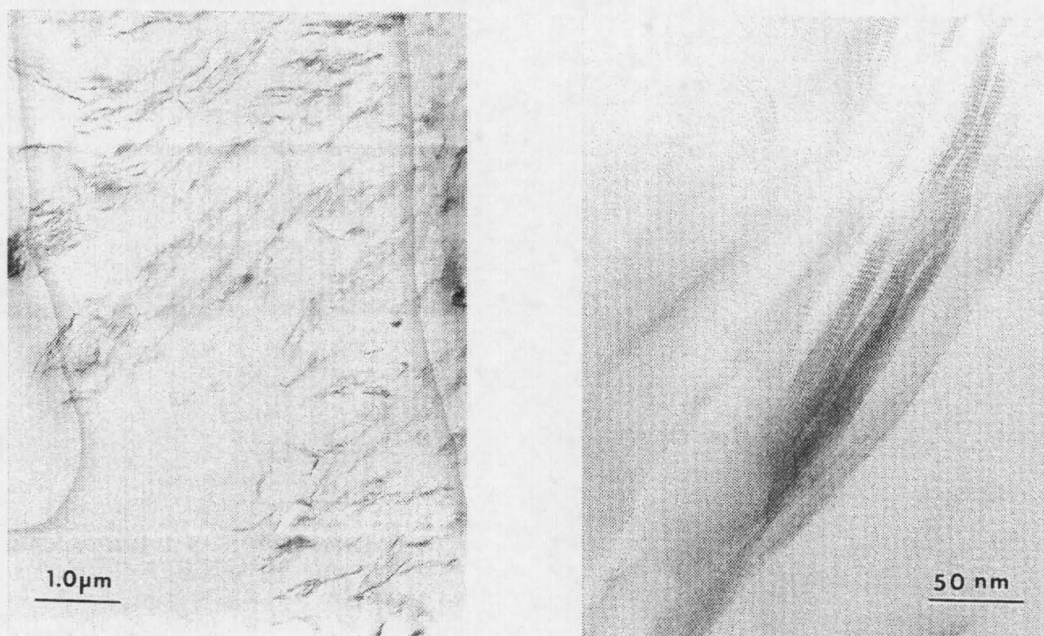


Fig 4. TEM images of the polystyrene nanocomposite of dicyclohexano-18-crown-6 potassium.

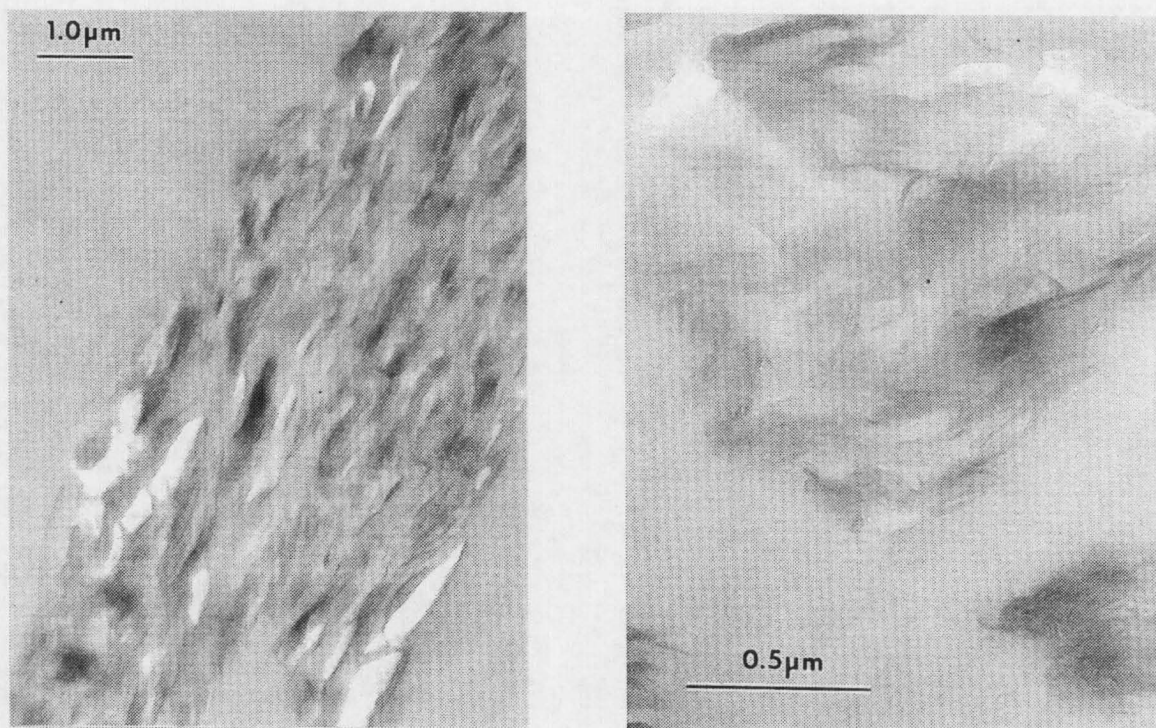


Fig. 5. TEM images for [2.2.2] cryptand sodium clay-polystyrene.

should be noted that both materials do not have good overall microdispersion; there are regions in these systems where no clay exists. Where clay does exist, it is either intercalated (dicyclohexano-18-crown-6 potassium clay), or a mixture of intercalated and exfoliated nanostructures (cryptand-sodium clay).

Thermogravimetric analysis. The thermal stability of all of the materials has been characterized by TGA. The results are collected in Table 3; this table shows the temperature at which 10% degradation occurs, $T_{0.1}$, a measure of the onset of the degradation, the temperature at which 50% degradation occurs, $T_{0.5}$, a

Table 3. Thermogravimetric Analysis for Polystyrene and the Blends and Nanocomposites With Various Chelated Clays, Mass Fraction of Clay Is 1%.

| Material | T _{0.1} , °C | T _{0.5} , °C | Char |
|--------------------|-----------------------|-----------------------|------|
| Polystyrene | 351 | 404 | 0 |
| PS-Na-cryptand | 383 | 411 | 2 |
| PS-K-cryptand | 383 | 411 | 3 |
| PS-K-18-crown-6 | 380 | 411 | 3 |
| PS-K-dibenzo | 382 | 406 | 3 |
| PS-K-benzo | 289 | 420 | 3 |
| PS-K-dicyclohexano | 400 | 443 | 3 |

measure of the mid-point of the degradation, and the fraction which is not volatile at 600°C, char. Except for the dicyclohexano-substituted potassium clay, there is only a small increase in both T_{0.1} and T_{0.5}, much smaller than what has been observed for other PS-clay nanocomposites (5, 8). The changes in the TGA for the dicyclohexano-clay nanocomposite are similar to what has been previously observed for organically-modified clay nanocomposites (5, 8). The TGA curves for the dicyclohexano-clay nanocomposite compared to virgin PS are shown in Fig. 6.

Cone calorimetry. The fire properties of the nanocomposite of *cis*-dicyclohexano-18-crown-6 potassium clay have been assessed by cone calorime-

try. The cone data are shown in Table 4. The peak heat release rate, PHRR, is an important term used to describe the effectiveness of a particular formulation. The heat release rate curve for PS, the dibenzo material, and the dicyclohexano nanocomposite are shown in Fig. 7. It is of interest to note that the dibenzo-clay, which according to XRD contains only a small amount of intercalated material, has a curve similar to that of the dicyclohexano, a completely intercalated material. Apparently the amount of intercalation and/or exfoliation in the nanocomposite has about the same effect on the heat release rate.

The nanocomposites invariably show a lowered peak heat release rate relative to the virgin polymer. In this instance, the reduction is in the range of 25%–30%. For comparison, the percentage reduction for PS-clay nanocomposites is about 50%, while in PMMA-clay nanocomposites the reduction was in the same range as observed for these crown ether complexes. The lower reductions observed for these PS nanocomposites compared to previous work may be due to the poorer nanodispersion with the crown ethers. The ignition occurs earlier than in the virgin polymer, an effect that has been previously observed with PS-clay nanocomposites (5, 8), but not in PMMA-clay system, in which the ignition takes place later than in the virgin polymer (17).

Fire retardancy in polymer clay nanocomposites has been attributed to the barrier properties that result from a concentration of the clay at the surface of the degrading polymer (4) and by paramagnetic trapping of radicals produced in the degradation by iron impurities in the clay (18). Both of these are possible explanations for the efficacy of these crown ether-containing nanocomposites.

CONCLUSION

Crown ethers have been used to modify both sodium and potassium clays, and the d-spacings of the clays in the presence of the crown ether increases by 0.5 to 1 nm. Complexation of the sodium clay by crown ethers does not permit the formation of nanocomposites, but they do form with the potassium clay, especially when complexed by dicyclohexano-18-crown-6. This has the highest complexation constant of all crowns that have been used in this study, and this complexation constant may be an important criterion controlling clay modification and nanocomposite formation. The thermal stability, as measured by thermogravimetric analysis, and the fire properties, as assessed by cone calorimetry, show that these systems have enhanced properties, similar to what has been observed with organically modified clays.

ACKNOWLEDGMENT

This work was performed under the sponsorship of the U.S. Department of Commerce, National Institute of Standards and Technology, Grant Number 70NANB6D0119.

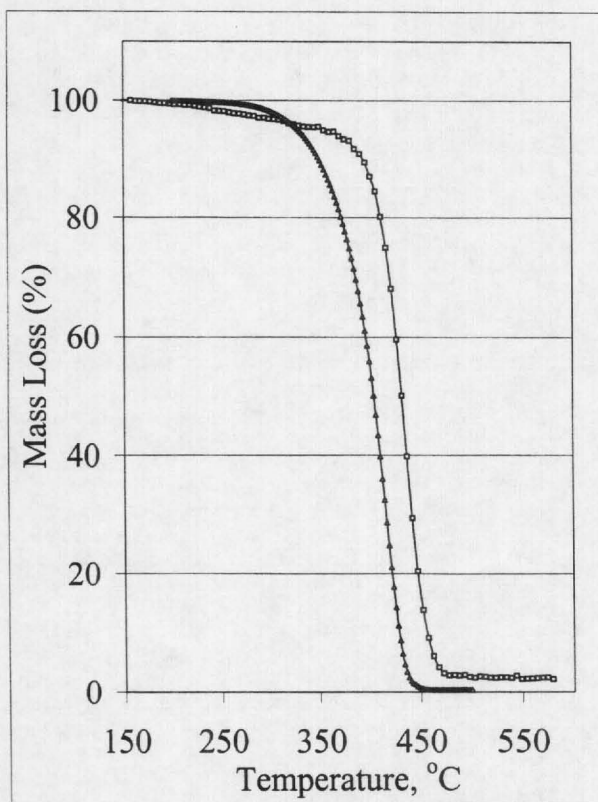


Figure 6. TGA curves of polystyrene, Δ and *cis*-dicyclohexano-18-crown-6 clay nanocomposites, \square .

Table 4. Cone Calorimetry Data of Polystyrene and Its Nanocomposites at 50 kW/m²; Mass Fraction of Clay Is 3%.

| Nanocomposite | T _{ignition} (S) | PHRR,* (kW/m ²) (% diff) ¹ | T _{PHRR} * (s) | Mean HRR* (kW/m ²) | ASEA* (m ² /kg) | AMLR* (g/s·m ²) |
|--------------------|---------------------------|--|-------------------------|-----------------------------------|-------------------------------|--------------------------------|
| PS | 42 | 1845 | 118 | 946 | 1265 | 35 |
| PS-K-dicyclohexano | 17 | 1397 (-24) | 106 | 794 | 1333 | 31 |
| PS-K-dibenzo | 33 | 1306 (-29) | 103 | 786 | 1335 | 31 |

¹ % diff = [P_{HRR}(no clay) - P_{HRR}(clay)] / P_{HRR} (no clay).

*T_{ignition}, time to ignition; PHRR, peak heat release rate; T_{PHRR}, time to peak heat release rate; Mean HRR, mean heat release rate; ASEA, Average Specific Extinction Area; AMLR: Average Mass Loss Rate.

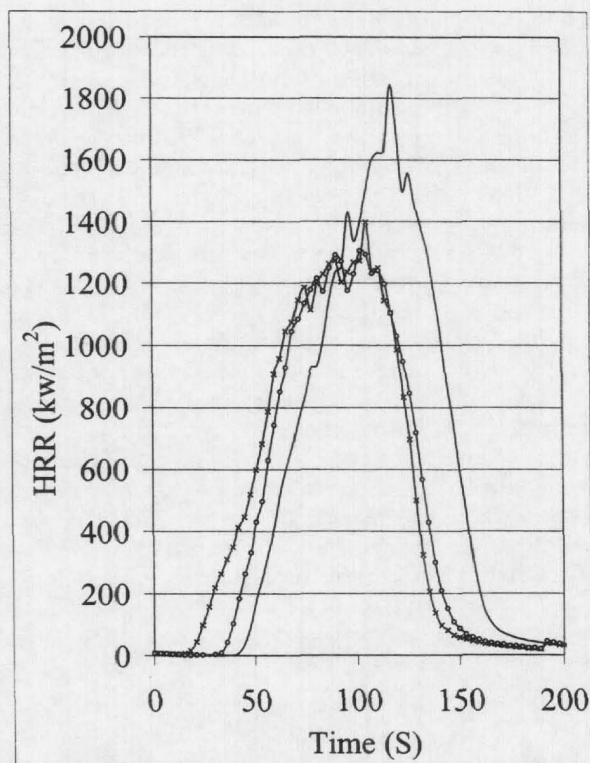


Figure 7. The heat release rate curves for polystyrene, —, the potassium dicyclohexano-18-crown-6 nanocomposite, X, and the potassium dibenzo-18-crown-6 nanocomposite, O.

LIST OF ABBREVIATIONS

- XRD: X-ray diffraction
 TEM: transmission electron microscopy
 TGA: thermogravimetric analysis
 PS: polystyrene
 PA-6: polyamide -6
 PS-Na-cryptand: polystyrene with sodium clay complexed with cryptand
 PS-K-cryptand: polystyrene with potassium clay complexed with cryptand
 PS-K-18-crown-6: polystyrene with potassium clay complexed with 18-crown-6
 PS-K-dibenzo: polystyrene with potassium clay complexed with dibenzo-18-crown-6

PS-K-benzo: polystyrene with potassium clay complexed with benzo-18-crown-6

PS-K-dicyclohexano: polystyrene with potassium clay complexed with dicyclohexano-18-crown-6

REFERENCES

- Y. Kojima, A. Usuki, M. Kawasumi, A. Okada, Y. Fukushima, T. Karauchi, and O. Kamigaito, *J. Mater. Res.*, **8**, 1185 (1993).
- Y. Kojima, A. Usuki, M. Kawasumi, A. Okada, Y. Fukushima, T. Karauchi, and O. Kamigaito, *J. Polym. Sci. Part A: Polym. Chem.*, **31**, 983 (1993).
- Y. Kojima, A. Usuki, M. Kawasumi, A. Okada, Y. Fukushima, T. Karauchi, and O. Kamigaito, *J. Polym. Sci. Part A: Polym. Chem.*, **31**, 1775 (1993).
- J. W. Gilman, T. Kashiwagi, E. P. Giannelis, E. Manias, S. Lomakin, J. D. Lichtenham, and P. Jones, in *Fire Retardancy of Polymers: The Use of Intumescence*, 201-221, M. Le Bras, G. Camino, S. Bourbigot, and R. Delobel, eds., Royal Society of Chemistry, London 1998.
- J. Zhu and C. A. Wilkie, *Polym. Int.*, **49**, 1158 (2000).
- T. Lan, P. D. Kaviratna, and T. J. Pinnavaia, *Chem. Mater.*, **6**, 573 (1994).
- R. A. Vaia, S. Vasudevan, W. Krawiec, L. G. Scanlon, and E. P. Giannelis, *Adv. Mater.*, **7**, 154 (1995).
- J. Zhu, A. B. Morgan, F. J. Lamelas, and C. A. Wilkie, *Chem. Mater.*, **13**, 3774-3780 (2001).
- M. Alexandre and P. Dubois, *Materials Science and Engineering*, **28**, 1 (2000).
- X. Kornmann, L. A. Berglund, and J. Sterte, *Polym. Eng. Sci.*, **38**, 1351 (1998).
- E. Ruitz-Hitzky and B. Casal, *Nature*, **276**, 596 (1978).
- P. Aranda, J. C. Galvan, B. Casal, E. Ruitz-Hitzky, *Electrochim. Acta*, **37**, 1573 (1992).
- J. W. Gilman, T. Kashiwagi, A. B. Morgan, R. H. Harris Jr., L. Brassell, H. W. Award, R. D. Davis, L. Chyall, T. Sutto, P. C. Trulove, and H. DeLong, *Proceedings of Additives 2001* (March 2001).
- J. W. Gilman, T. Kashiwagi, M. Nyden, J. E. T. Brown, C. L. Jackson, S. Lomakin, E. P. Giannelis, and E. Manias, in *Chemistry and Technology of Polymer Additives*, pp. 249-265, S. Al-Malaika, A. Golovoy, and C. A. Wilkie, eds., Blackwell Scientific, 1999.
- G. W. Gokel, *Crown Ethers and Cryptands*, Royal Society of Chemistry, Cambridge, U.K. (1991).
- M. Zanetti, G. Camino, D. Canavesse, A. B. Morgan, F. J. Lamelas, and C. A. Wilkie, *Chem. Mater.*, in press.
- J. Zhu, P. Start, K. A. Mauritz, and C. A. Wilkie, *Polym. Degrad. Stab.*, in press.
- J. Zhu, F. M. Uhl, A. B. Morgan, and C. A. Wilkie, *Chem. Mater.*, **13**, 4649-4654 (2001).